International Journal of Plasticity 174 (2024) 103894



Contents lists available at ScienceDirect

International Journal of Plasticity

journal homepage: www.elsevier.com/locate/ijplas





Optimization of crystal plasticity parameters with proxy materials data for alloy single crystals

Shahram Dindarlou [a], Gustavo M. Castelluccio [b,*]

[a] University of Twente, Netherlands
[b] School of Aerospace, Transport and Manufacturing, Cranfield University, Cranfield, UK

ARTICLE INFO

Keywords:
Crystal plasticity
Parameter uncertainty
Parameters optimization
Material independent parameters
Polycrystal fitting

ABSTRACT

Multiscale modeling approaches have demonstrated ample value in understanding, predicting, and engineering materials response. While increasing computational power has aided in modeling atomic behavior from first principles, modeling mesoscale mechanisms such as intergranular failure or crack initiation still rely strongly on correlative models. Crystal Plasticity models have been extensively used to relate process-property-structure in metallic materials including mesoscale effects such as texture, microplasticity, and failure variability. However, models still suffer from low predictive power at the grain scale, which leads to poor damage prognosis outside the experimental calibration set. In addition to model form error, mesoscale uncertainty is dominated by an inadequate model parameterization that arises from calibration exclusively to macroscopic experimental data. This work explores parameter uncertainty in Crystal Plasticity models and proposes a hybrid physic-based and numerical optimization approach to identify parameters associated to mesoscale strengthening in FCC metals and alloys. The strength and novelty of the approach rely on calibrating parameters independently using single-crystal and polycrystal stress–strain curves. We further demonstrate that multiple materials can be incorporated simultaneously into a single optimization algorithm to robustly quantify mesoscale material-invariant parameters. These values are then used to blindly predict the response of single- and poly-crystals engineering alloys. As a result, our approach mitigates modeling uncertainty by augmenting the data for calibration with single crystal experiments from different materials with similar dislocation structures (i.e., proxy materials). The results provide the basis for a robust parameterization of crystal plasticity models that can predict single- and poly-crystal responses for engineering alloys even in the absence of direct experimental data.

1. Introduction

The inelastic response of engineering metallic materials cannot yet be predicted sole from first principles and engineers rely on strongly correlative models that are informed by myriads of experimental tests. These data-driven approaches require testing every material under numerous abnormal extreme service conditions, which can be costly, impractical, or even impossible for some service conditions. Alternatively, mechanistic approaches such as crystal plasticity (CP) (Roters et al., 2010) can predict the constitutive response of metallic materials from a number of principles, but they require adequate parameterization to avoid spurious extrapolations and low predictive power at the grain scale (mesoscale) (Pokharel et al., 2014) .

* Corresponding author.
E-mail address: castellg@cranfield.ac.uk (G.M. Castelluccio).

https://doi.org/10.1016/j.ijplas.2024.103894
Received 17 November 2023; Received in revised form 17 January 2024
Available online 28 January 2024
0749-6419/© 2024 The Author(s). Published by Elsevier Ltd. This is an open access article under the CC BY license (http://creativecommons.org/licenses/by/4.0/).

Researchers have normally advanced constitutive models with novel physics-inspired formulations that often lack equally rigorous quantification of parameter uncertainties (Roy and Oberkampf, 2011) . However, models without unique and independent parameters cannot capture unequivocally the local response at or below the grain scale (El Shawish and Cizelj, 2017; Pirgazi and Kestens, 2021) . Optimization and artificial intelligence schemes that fit parameters only to macroscopic stress–strain curves (Sedighiani et al., 2022; Herrera-Solaz et al., 2014) are prone to overfitting and simply lack grain-level information. Since mathematical optimization does not address the dearth of data that hinders independent parameterization, the solution lies in the fusion of data from different sources and scales (Sangid, 2020). For example, Knezevic and coworkers (Savage et al., 2021; Feng et al., 2022; Veasna et al., 2023) developed approaches to parameterized CP models that predict texture evolution by integrating stress–strain curves from different loading conditions as well as information from grain rotation and phase formation (e.g., twins). Their work clearly demonstrates that proper parameterization of CP to predict texture requires a plethora of data across scales.

Other researchers (Estrin et al., 1996; Brahme et al., 2011; Steckmeyer et al., 2012; Sauzay et al., 2014) sought multiscale data augmentation by parameterizing the morphology of sessile dislocation substructures characterized by microscopy. Castelluccio and coworkers (Castelluccio and McDowell, 2017; Dindarlou and Castelluccio, 2022; Ashraf and Castelluccio, 2023) further extended this approach and garnered the mechanics of dislocation structures to propose a substructure-sensitive CP based on a two-phase material model (i.e., walls and channels). Their work proved the need for validating models to single crystal responses by presenting different parameterizations that match polycrystalline stress–strain curves accurately but differ drastically for single crystals. Other researchers have also highlighted the value of parameterizing with experimental data from deforming a single grain or crystal (Venkatraman et al., 2022; Bertin et al., 2013). Parameterizations that predict macroscopic polycrystal but not single crystal responses translates into grain-level error (Sangid, 2020) and leads to poor damage prognosis (Rovinelli et al., 2017).

Two main limitations currently exist in mitigating model input errors (Roy and Oberkampf, 2011): firstly, most CP models have not been validated with single crystal experiments and the literature lacks specific optimization approaches to integrate these data. Secondly, single crystal data are scarce and despite some recent advances (Lodh et al., 2023), they are unlikely to be available for most engineering materials. Hence, this work addresses both problems with a novel multi-objective physics-based optimization approach that estimates unique material-invariant parameters for FCC metals by calibrating parameters to single- and polycrystal responses. We study parameter sensitivity by performing separate optimization routes using individual or collective data from Cu, Ni and Al to blindly predict the single-crystal response of engineering alloys. We propose a novel approach to calibrate CP models with single- and poly-crystal data, and we demonstrate the value material-invariant parameters to mitigate uncertainty when no single-crystal data is available.

1.1. Uncertainty in calibrating exclusively to polycrystal data

Strain hardening in metallic materials arises from multiple cooperating mechanisms across scales (point defects, forest dislocations, grain boundaries, etc.). Many of these strengthening mechanisms result in similar macroscopic observable effects, which makes it difficult to distinguish their origin, particularly for polycrystalline materials. The analysis of single crystals supports the understanding of mechanisms by avoiding grain boundaries and promoting different dislocation processes among different orientations. Hence, validating CP models with numerous single crystals mitigates epistemic and aleatoric uncertainty of forest dislocation hardening. However, the main drawback is the lack of single crystal experimental data, which are only typically available for a few pure metals.

To demonstrate the magnitude of the uncertainty associated with calibrating models only to polycrystalline experiments, we consider the substructure-sensitive CP model (Dindarlou and Castelluccio, 2022) described in the supplementary material, which is capable of predicting single crystal responses. Details about the mesh, loading conditions, boundary conditions and microstructure are also presented in the supplementary material. In this case, we computed the parameters for stainless steel from the polycrystal data in Fig. 1 along with the optimization procedure based on the Levenberg–Marquardt method as proposed by Herrera-Solaz et al. (2014). This numerical approach estimates the parameters by minimizing an Euclidean objective function between the experimental and the predicted stress–strain curve.

Fig. 1(a) demonstrates that the CP model with the optimized parameters closely matches the polycrystal experimental data. In comparison, Fig. 1(b) presents CP single crystals predictions along with the experimental results from Karaman et al. (2001) and Kashyap and Tangri (1995), who performed rare testing of stainless steels. In this case, the model results in incredibly poor performance in predicting single crystal response. Indeed, not only the [111]-crystal hardening is underestimated, but the [213] crystal artificially hardens above all curves at a strain of about 10%. These inaccuracies are typical in CP models parameterized only with macroscopic polycrystal stress–strain data and arise from an artificial compensation in hardening among different crystals (excessive strength for [213] compensates for [100] and [111] deficits). As demonstrated later, such poor prediction power is due to the model inputs rather than model forms. In any case, most CP models are not systematically validated with single crystal data, which tends to result in low predictive power at the grain level and is problematic for predicting mechanisms such as grain boundary impingement, strain localization, decohesion, and cracking.

2. Methodology

Our premise for mitigating model uncertainty, particularly in relation to CP models with numerous material parameters, is to reduce the number of parameters to facilitate their independent estimation in sequence. The demonstration of the optimization sequence considers the substructure-sensitive CP model for monotonic loading (Dindarlou and Castelluccio, 2022) (full model

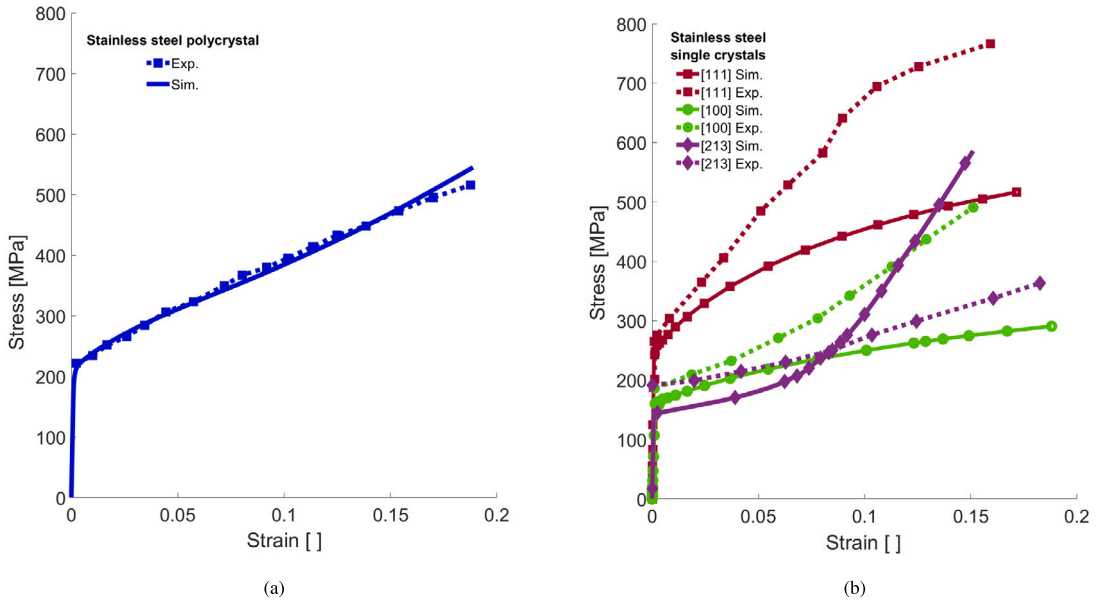


Fig. 1. Prediction of stress–strain curves of stainless steel (316) using the parameters optimized by fitting with polycrystal data. While the polycrystal fitting is excellent, the parameters fail to predict single crystals, which indicates that optimization with polycrystal data may not guarantee the predictability for single crystals.
Source: Experiments from Refs. Karaman et al. (2001) and Kashyap and Tangri (1995).

description available in the supplementary material) with the understanding that the strategy is applicable to other approaches. Substructure-sensitive approaches by Castelluccio and co-authors (Dindarlou and Castelluccio, 2022; Ashraf and Castelluccio, 2023) were designed to allow for the independent validation of mesoscale attributes—dislocation structure spacing (d_{struct}), aspect ratios (η), wall fractions (f_w)—using TEM or ECCI imaging. The approach estimates d_{struct} with the inverse of the local (i.e., discounting long-range effects) shear stress (τ^{α}) associated with a slip system α through the similitude principle, i.e.,

$$d_{struct} = \frac{\mu b}{\tau^{\alpha}}, \tag{1}$$

which depends on a material- and temperature-independent parameter (Sauzay and Kubin, 2011). Moreover, the algorithms predict η and f_w for arbitrary crystal orientation to reproduce the response of single- and poly-crystalline. Although f_w and η algorithms are different for monotonic and cyclic loading, in both cases, the associated parameters are material-invariant (i.e., FCC materials share identical mesoscale parameters). Despite the success of these models, prior efforts fell short of a rigorous optimization of mesoscale parameters that match macroscopic and mesoscopic experiments with minimum mathematical error. Moreover, a robust optimization approach further serves to validate the notion of material invariance with respect to specific subsets of parameters.

Fig. 2 summarizes the novel optimization approach, which consists of four steps, each one running an optimization algorithm proposed by Herrera-Solaz et al. (2014) to fit parameters to different experimental data. Step I relies on yield stress data, Steps II and III employ stress–strain curves from a single crystal that develop thermal and athermal dislocation structures (Ashraf and Castelluccio, 2022), respectively, and Step IV relies on the polycrystal stress–strain curve. Steps II to IV are calibrated to curves with at least 10% deformation to achieve saturation of dislocation structures (Dindarlou and Castelluccio, 2022). We highlight that subsequent steps do not affect prior parameters and do not reuse prior data.

2.1. Pre-optimization step

Prior to optimization, we recognize that a number of CP parameters can be effectively estimated independently from the literature. For example, elastic constants can be inferred accurately from atomistic modeling or experiments as well as the Burgers vector, whose uncertainty only results in a second-order effect in CP results. As discussed by Sauzay and Kubin (2011), the dislocation self-interaction coefficient can be assumed to be $\alpha_{ii} \sim 0.1$ for numerous materials based on independent estimations with dislocation dynamics modeling and experiments. The uncertainty of this coefficient is intrinsically related to the estimated initial dislocation density and the model form error (Oberkampf et al., 2002) for the dislocation mean free path (Devincre et al., 2008). Hence, we choose a predetermined value for α_{ii} and we will consider well-annealed FCC materials with large grains (>100 μm) and low initial dislocation densities (10^{11} m^{-2}) to avoid spurious calibrations that compensate for the other errors, as proposed by Ashraf as Castelluccio (Ashraf and Castelluccio, 2021). Another low-sensitivity parameter corresponds to the jump frequency, which is

typically in the range between 10^{10} and 10^{13} s^{-1} and is closely related to the atomic vibration. Here, we consider the atomic attempt frequency from Eyring's reaction rate theory as employed by Ashraf and Castelluccio (2021), i.e.,

$$\nu = \frac{k_B T}{h}, \tag{2}$$

in which is T is the temperature, and k_B and h are the Boltzmann and Plank constants, respectively. Furthermore, the initial values for parameters in Steps II to IV correspond to earlier estimates (Dindarlou and Castelluccio, 2022).

2.2. Step I: Yield stress

First, we estimate the parameters that describe the dislocation glide energy barrier associated with atomic unit processes (e.g., solid solution strengthening from point defects, interstitial or substitutional alloying, and small precipitates compared to dislocation lengths). Numerous formulations (Langer, 2019; Dunne et al., 2007; Kocks et al., 1975) have been proposed to parameterize the Gibbs free energy associated with dislocation glide. Here, we consider the traditional approach by Kocks et al. (1975), with the understanding that the optimization would serve other formulations. Kocks proposed Arrhenius-type equation such that,

$$\dot{\gamma}^{\alpha} = \rho^{\alpha} b \nu \eta d_{struct} \exp\left(-\frac{F_0}{k_B T} \left\langle 1 - \left[\frac{\langle \tau^{\alpha} \rangle}{s_t^0 \frac{\mu}{\mu_0}} \right]^p \right\rangle^q \right), \tag{3}$$

in which the plastic shear rate ($\dot{\gamma}^{\alpha}$), depends on the dislocation density (ρ^{α}). Plastic shear is controlled by four parameters: glide activation energy at 0 K (F_0), the thermal stress, (s_0), and profile parameters p and q. Furthermore, μ and μ_0 are the shear modulus at temperature T and 0 K, respectively.

As discussed by Ashraf and Castelluccio (2021), Gibbs free energy parameters are not uniquely defined when fitted to experimental stress–strain curves at a single temperature or strain rate. In practical terms, this means that an increase in F_0 can be compensated by a decrease in s_0 to match the experiments performed at one temperature or strain rate. However, this ambiguity gets resolved when calibrating with experiments at multiple experimental temperatures. Ashraf and Castelluccio (2021) went further and gathered experimental data across temperatures for multiple FCC materials to demonstrate that for fixed $p = \frac{2}{3}$ and $q = \frac{3}{2}$, F_0 correlates inversely with the material stacking fault energy (SFE), i.e.,

$$F_0 \sim 2.6 - 0.0067 * \frac{SFE}{\text{mJ m}^{-2}}, \tag{4}$$

The robustness of this approach relies on the simultaneous evaluation of multiple materials rather than a single experimental set, and the outcomes are parameters estimated independently. Hence, s_t^0 is the only unknown parameter and we can optimize its value such that CP simulations match the yield point of polycrystal experiments with the understanding that single crystal data would also serve this purpose if they were available. We note that the role of dislocation densities on yield strength is negligible for large-grain well-annealed engineering materials. Furthermore, the energetics of dislocation glide is independent of the loading conditions, and indeed this approach was successfully applied for calibrating glide activation parameters under cyclic loading (Ashraf and Castelluccio, 2023).

2.3. Step II: Thermal structures

Next, we calibrate the parameters associated with thermal dislocation structures (equiaxed cells) by employing stress–strain curves from crystal orientated for profuse cross-slip (e.g. [111]). As shown by Knoesen and Kritzinger (1982) for monotonic loading and by Ashraf and Castelluccio for cyclic loading (Ashraf and Castelluccio, 2022), these crystal orientations result in well-defined equiaxed cells (Type III structure) driven by cross slip and their wall fractions are constant and independent of temperature. Hence, we employ the numerical optimization algorithm (Herrera-Solaz et al., 2014) to optimize the wall fraction value for cells f_w^{III} and the similitude coefficient K_{struct} discussed by Sauzay and Kubin (2011). The morphology of cells results in an equiaxed structure with an aspect ratio of $\eta^{III} = 1$ and does not require calibration. Because thermal structures have constant wall fractions, forest dislocation hardening in substructure-sensitive CP models (Dindarlou and Castelluccio, 2022; Ashraf and Castelluccio, 2023) depends on the refinement of the cell size.

2.4. Step III: Athermal structures

Next, we calibrate the saturation values for the mesoscale parameters related to Type I and II thermal structures, which correspond to elongated cells. We assume ($f_w^I = f_w^{II}$ and $\eta^I = \eta^{II}$) and employ the numerical algorithm to optimize the parameters using experimental data from single crystals oriented to prevent cross slip (which limits wall fraction refinement with temperature). Because athermal structures vary their wall fractions, forest dislocation hardening depends on the simultaneous refinement of the wall thickness, cell size, and aspect ratio until reaching saturation approximately at 10% strain

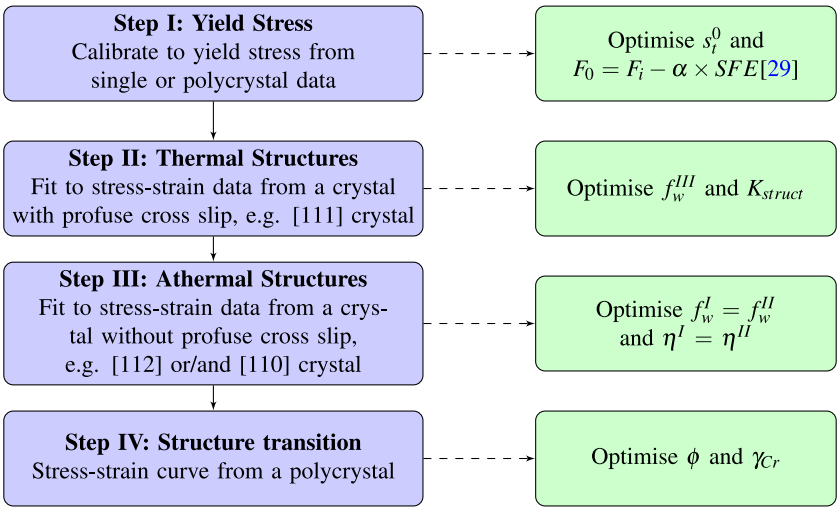


Fig. 2. Sequential physics-based CP parameters optimization for FCC materials. Stress–Strain curves for Steps II to IV should reach at least 10% to achieve saturation of the dislocation structures (Dindarlou and Castelluccio, 2022).

2.5. Step IV: Structure transition

Finally, we estimate γ_{cr}, which controls for intermediate crystal orientations the transition from athermal into thermal structures with increasing accumulated cross slip. Because this condition would require assessing numerous crystal orientations, we calibrate γ_{cr} using polycrystal experimental data to capture the transformation of enough grains to equiaxed cells. We also optimize the cross slip efficiency, ϕ, which controls the annihilation and production of dislocation density.

3. Results and discussion

3.1. Pure metals

The proposed physics-based optimization methodology sequentially quantifies different CP parameters independently to match single- and poly-crystals. Fig. 3 exemplifies the results from the optimization sequence applied to Cu. The optimization relies on the stress–strain curves from two crystal orientations with and without profuse cross slip, which results in thermal and athermal structures, respectively (Ashraf and Castelluccio, 2022). Each subfigure in Fig. 3 presents an optimization step and includes the experimental data used for calibration (triangle gray line), intermediate optimization predictions (short broken red line), and the optimum solution (long broken green line). These results show that the model form and the parameterization adequately capture the experimental responses of single- and poly-crystals.

Following an identical procedure, we optimized the parameters for Ni and Al, and results in Table 1 demonstrate that mesoscale parameters (K_{struct}, f_w, η) are almost identical among all the materials. Also, cross-slip parameters are closely related, which suggests that a similar amount of accumulated cross-slips is required to create similar structures in different materials; the caveat is this cross-slip amount will occur at different strain levels for different materials. The similarity of these values supports the notion that material invariant parameters characterize forest dislocation hardening in FCC metals and the differences in Table 1 are due to overfitting. Moreover, the values are in close agreement with the estimates from inspection of dislocation structures in TEM and SEM micrographs (Dindarlou and Castelluccio, 2022), which supports that calibration to single crystals dislocation structures provides a mesoscale validation.

By assuming that different materials have identical mesoscale material invariant parameters, we implemented a multi-objective physics-based optimization approach that combines Cu, Ni, and Al single- and poly-crystal stress–strain curves. This approach uses the experimental data across multiple materials to optimize the parameters that best match all the experiments simultaneously. As a result, we effectively mitigate experimental uncertainty from single- and poly-crystal samples. Fig. 4 presents the CP predictions for single- and poly-crystals for Cu, Ni, and Al from a single multimaterial parameters optimization. We emphasize that all modeling predictions use the same mesoscale parameters presented in the last column of Table 2, and they only differ on the elastic constants, the activation energy F_0, and the athermal stress s_0.

3.2. Calibration of engineering alloys by material proxy

Experiments (Hansen et al., 2008; Li et al., 2011) have shown that FCC metals and engineering alloys at equal homologous temperatures share similar dislocation structures, which induce equivalent strain hardening among these materials. This logic

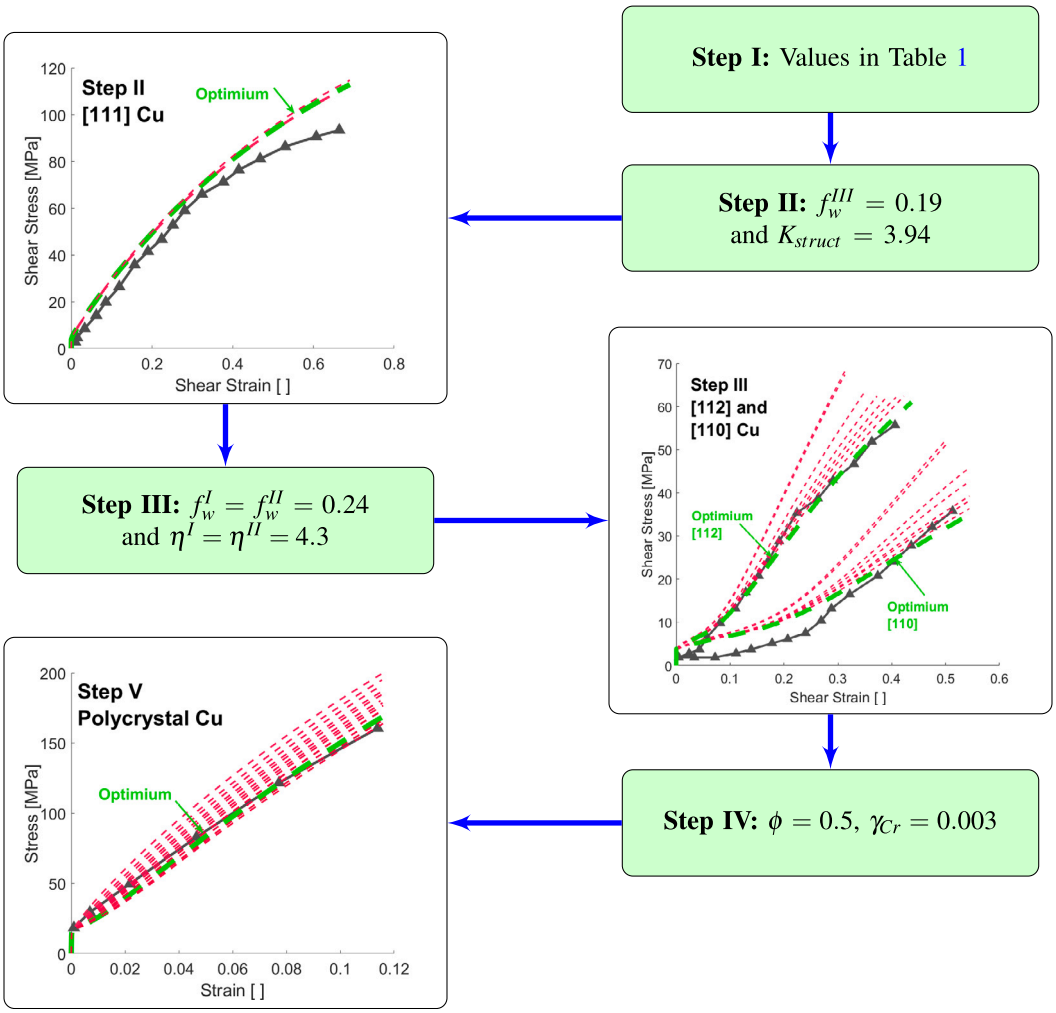


Fig. 3. Sequential physics-based parameter optimization using experimental data from Cu. Red curves are predictions with non-optimized parameters and show the optimization path and green lines are predictions with optimized parameters. (For interpretation of the references to color in this figure legend, the reader is referred to the web version of this article.)
Source: Gray points experimental data taken from Refs. Takeuchi (1975), Venkatesan and Beshers (1970), Follansbee and Gray (1991), Mukherjee et al. (1965) and Tagami et al. (2001).

Table 1
Parameters of various FCC materials optimized independently.

Parameter	SS 316 (poly)	Cu	Ni	Al
s_t^0, MPa	250	8	20	10
SFE, mJ m^{-2}	78 (Schramm and Reed, 1975)	46 (Devlin, 1974)	120 (Carter and Holmes, 1977)	166 (Murr, 1973)
$F_0 = F_i - \alpha \times SFE$ (Ashraf and Castelluccio, 2021), $\frac{\text{kJ}}{\text{Mole}}$	180	155	145	80
K_{struct}	6	3.94	4.05	4.9
$f_w^I = f_w^{II}$	0.3	0.24	0.25	0.25
f_w^{III}	0.1	0.19	0.19	0.19
$\eta^I = \eta^{II}$	5	4.3	5	2.8
ϕ	0.5	0.48	0.49	0.49
γ_{Cr}	3^{-3}	3^{-3}	1^{-3}	3^{-3}
C_{11}, GPa	232.8	166.1	249.0	114.8
C_{12}, GPa	154.0	119.0	155.0	62.0
C_{44}, GPa	118.0	75.6	114.6	31.0

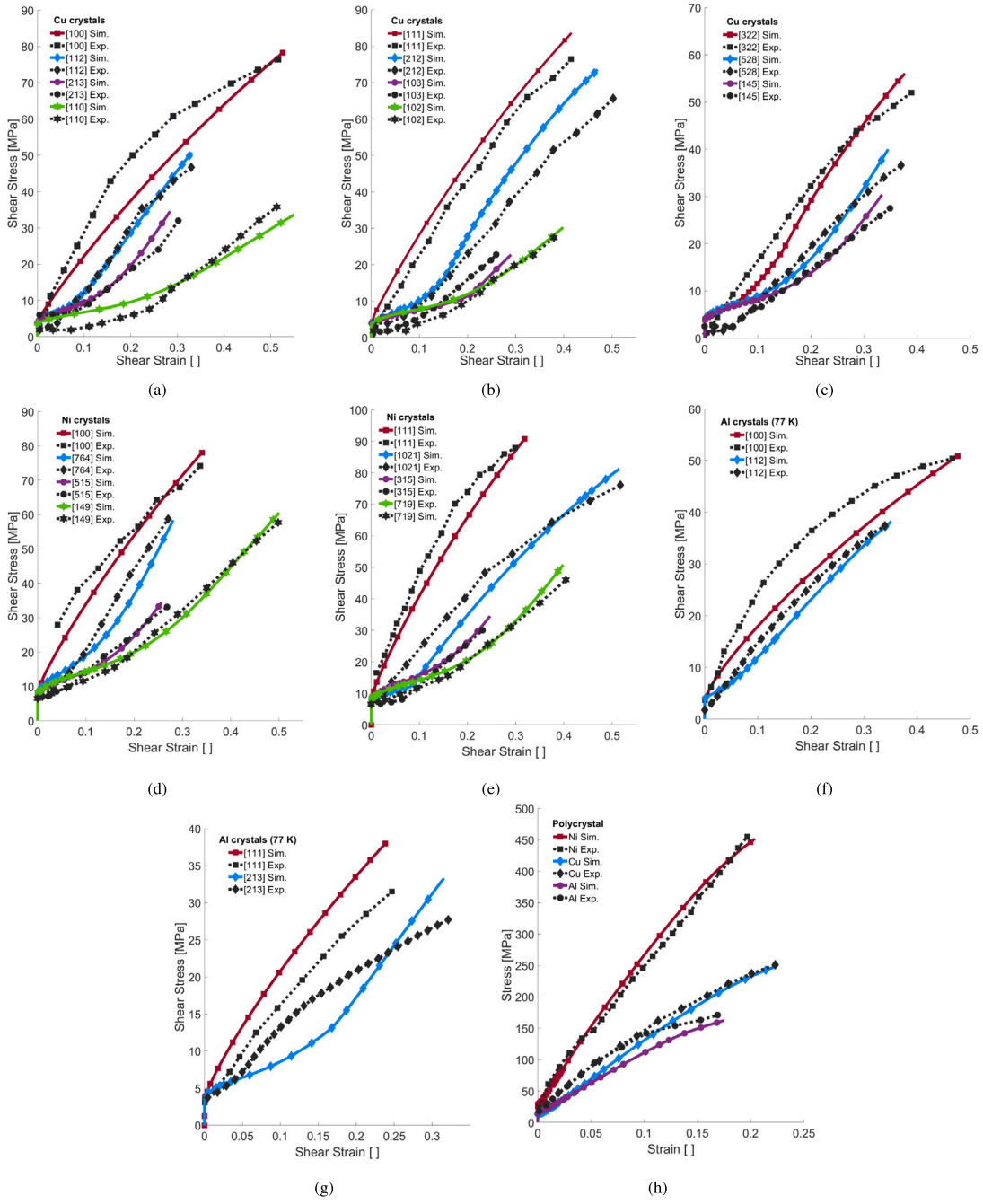


Fig. 4. Predictions of Cu, Ni, and Al single- and poly-crystals with only one unique set of parameters, optimized by combining experimental data from Cu, Ni, and Al (parameters in Table 2). Material invariant parameters enable the prediction of FCC materials, using experimental data from other materials for calibration (without the need for experimental testing).
Source: Experiments of Cu from Refs. Takeuchi (1975), Steeds (1966), Kawasaki (1974) and Heinrich et al. (1992), Ni from Refs. Venkatesan and Beshers (1970) and Follansbee and Gray (1991), Al from Refs. Mukherjee et al. (1965) and Tagami et al. (2001) and polycrsyals from Refs. Carreker and Hibbard (1953), Gracio et al. (1989), Thompson (1977) and Marnier et al. (2016).

supports using single crystal data available for pure metals as proxies to calibrate engineering alloys, for which we lack single crystal tests. Hence, we implemented Step I and IV of the optimization sequence using polycrystalline stress–strain data, while relying on the prior parameterization with Cu, Ni, and Al single crystals for Steps II and III (Table 2).

Fig. 5 presents the predictions for single- and poly-crystals for engineering alloys using the mesoscale parameters calibrated by combining data from multiple materials in Table 2. We emphasize that only elastic constants, F_0, s_t^0, and γ_{Cr} were different among

Table 2
Optimized parameters combining Cu, Ni, and Al experimental data. These parameters are employed to predict various engineering alloy responses.

Parameter	Cu, Ni, and Al combined
K_{struct}	4.05
$f_w^I = f_w^{II}$	0.24
f_w^{III}	0.19
$\eta^I = \eta^{II}$	4.5
ϕ	0.5
γ_{Cr}	3^{-3}

Table 3
Material parameters optimized by the proposed method for the alloys.

Parameter	SS 316	HEA	NiCr	NiCo	CuMn
s_t^0, MPa	250	150	20	20	8
SFE, mJ m^{-2}	78 (Schramm and Reed, 1975)	30 (He et al., 2014)	120 (Carter and Holmes, 1977)	120 (Carter and Holmes, 1977)	46 (Devlin, 1974)
$F_0 = F_t - \alpha \times SFE$ (Ashraf and Castelluccio, 2021), $\frac{\text{kJ}}{\text{Mole}}$	180	200	145	145	155
C_{11}, GPa	232.8	172.0	249.0	249.0	166.1
C_{12}, GPa	154.0	107.0	155.0	155.0	119.0
C_{44}, GPa	118.0	92.0	114.6	114.6	75.6

materials and only two parameters were fit—elastic constants were taken from the literature Table 3 and F_0 was estimated following the correlation with stacking fault energy (SFE) as proposed by Ashraf and Castelluccio (2021).

By relying on material-invariant parameters, the response of single- and polycrystal alloys only requires optimization of s_t^0 and γ_{Cr} in Steps I and V, respectively. Both optimizations can be done with polycrystal data while the approach still predicts single crystals. Interestingly, the polycrystalline material predictions in Figs. 5(f) and 5(g) do not match perfectly the experiments as compared to Fig. 1(b), which can be taken as a measure of the model form error (or prior overfitting). Certainly, the current CP model assumes no texture, low initial dislocation densities, and large grains to avoid size effects, which are sources of errors that can be mitigated without changing the model parameters. Thus, the systematic assessment of model input error and the avoidance of overfitting can effectively be used to understand model form error.

3.3. Sources of parameterization uncertainty

Although parameterization to polycrystals is not sufficient to assure mesoscale predictive power (Fig. 1), single crystal experiments bring larger uncertainty. For example, Fig. 6 presents one experimental result for Ni reported close to [8111] single crystal (Venkatesan and Beshers, 1970; Follansbee and Gray, 1991; Akhtar and Teghtsoonian, 1971) along with our modeling prediction using material invariant parameters (broken blue line), which does not match the experiments. However, a slight modification of one parameter (γ_0^{eq}) was sufficient to produce an excellent fitting to experiments (the dotted red line in Fig. 6(a)). The analysis of only these data suggests that the multimaterial parameterization validated in Fig. 5 is incorrect. However, the comparison of the experimental data with independent experimental data in Fig. 6(b) demonstrates that the orientation is incorrectly estimated on the original reference. This idea is further supported by TEM analysis of the dislocation structure aspect ratio (η) shown in Fig. 6(c), which is only predicted by material invariant parameters. In reality, the incorrect parameter provides additional hardening by assuming that cell structures appear at smaller strains (lower γ_0^{eq}). This response is analogous to that observed after rotating the sample towards the 001 orientation, which develops cells at lower due to the increase in cross slip. Hence, with a change in orientation or γ_0^{eq} we can reproduce the same macroscopic stress–strain response, but the latter option will not be predictive for other crystal orientations.

The variability in Fig. 6 exemplifies the sensitivity of stress–strain curves to the effective crystal misalignment (i.e., the orientation of the lattice with respect to the applied force direction after manufacturing and mounting the sample on the testing machine). It also demonstrates that small spurious modifications in parameters may be able to reproduce the experiment even when they are inaccurate. In this case, an incorrect parameter results in cell structures arising at smaller strains (which shortens Stage I), which resembles a rotation towards [001] orientation, for which cells develop at smaller strains compared to single slip or [011] orientations. Thus, rather than relying on one experiment, the overall uncertainty can be mitigated with the simultaneous calibration of CP parameterization with multiple single crystals.

To further assess the impact on the parameterization of single crystal misalignment, we present the results from the CP model calibrated for Ni, but adding five-degree random rotation, which is often used as a threshold for differentiating crystal orientations among grains. The results in Fig. 7 demonstrate that [110] crystals are less sensitive to misalignment, which can increase or decrease

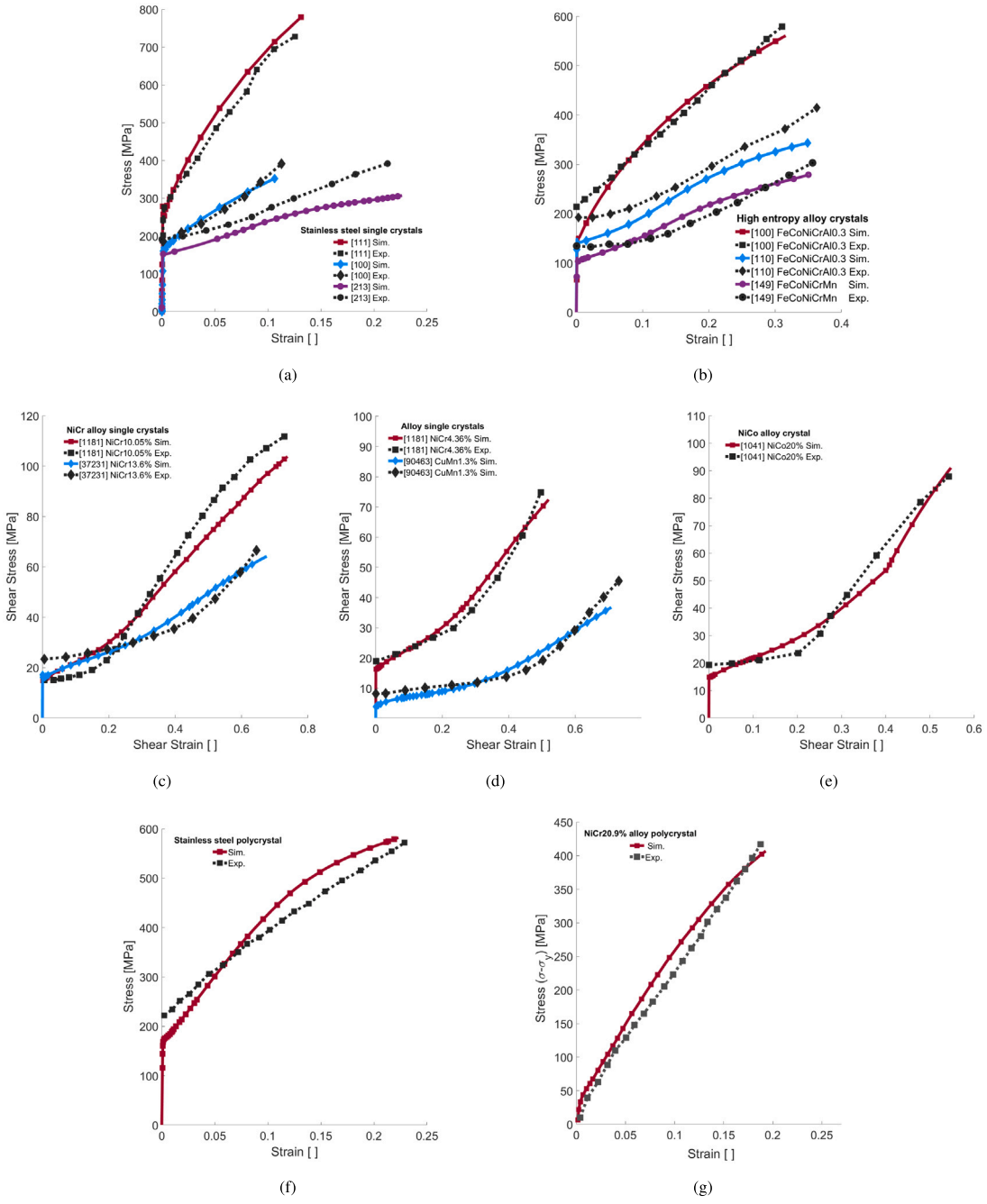
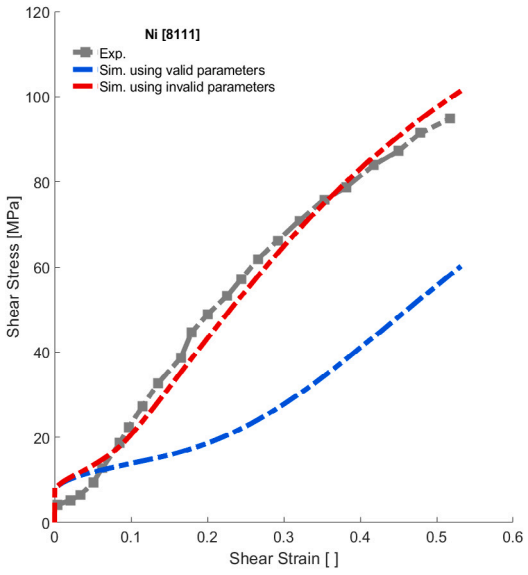
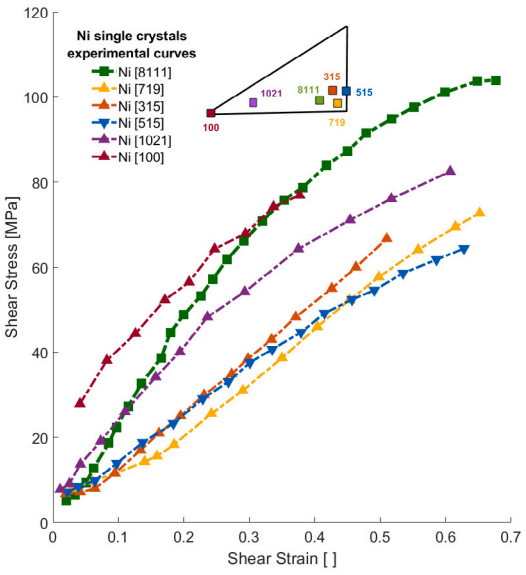


Fig. 5. Predictions of FCC alloys from optimized parameters using combined data from various FCC pure metals experimental data for calibration (Cu, Ni, and Al). Material invariant parameters optimized by the proposed approach enable the prediction of FCC alloys without experimental test requirements.
Source: Experiments from Refs. Karaman et al. (2001), Kashyap and Tangri (1995), Akhtar and Teghtsoonian (1971), Heinrich et al. (1992), Kronmüller (1959), Kireeva et al. (2018) and Kireeva et al. (2016).

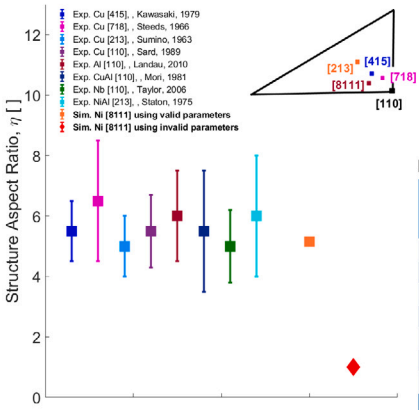
the hardening. On the contrary, the misalignment induces softening in orientations that promote cross slip ([100] and [111]), and the model results become an upper bound. These considerations should be taken into account by enlarging the calibration sampling with multiple crystals, especially for orientation that facilitates cross-slip. In addition to the effective misalignment between the lattice and load direction, minor misorientation within samples and different initial dislocation densities amplify testing uncertainties. These considerations put into perspective the quality of the results in Fig. 5 and suggest that an accurate model would not match all single crystal experiments given their intrinsic experimental uncertainty.



(a)



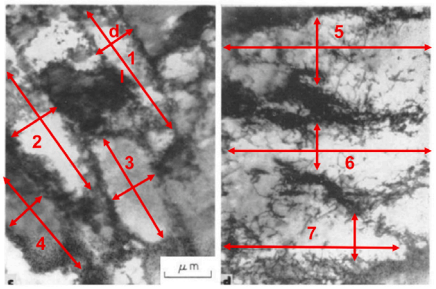
(b)



(c)

[110] Cu Crystal (Sard, 1989)

Cell No.	Dislocation structure aspect ratio measurement		
	l (μm)	d (μm)	$\eta = l/d$
1	4.0	0.8	5
2	5.5	1.1	5
3	4.0	1.0	4
4	5.0	1.0	5
5	6.0	1.2	5
6	0.54	0.9	6
7	5.0	1.0	5
Average			5.0



(d)

Fig. 6. (a) Predictions of Ni [8111] crystal using valid and invalid ($\gamma_0^{eq} = 40.0$) sets of parameters. Excellent fitting with invalid parameters shows that using only stress–strain curves for parameter optimization does not necessarily imply valid parameters and extra validation is required. (b) Experimental stress–strain curves for other Ni crystals in the neighborhood of [8111]. (c) Mesoscale structure of FCC crystals in the neighborhood of [8111] and (d) Measurement of structure aspect ratio from TEM images shown in c. Both macroscopic curves and mesoscale structures show that the experimental [8111] curve in a is may be incorrect. (For interpretation of the references to color in this figure legend, the reader is referred to the web version of this article.)
Source: Experiments from Refs. Venkatesan and Beshers (1970), Follansbee and Gray (1991), Akhtar and Teghtsoonian (1971), Kawasaki (1979), Steeds (1966), Sumino et al. (1963), Sard and Weil (1970), Landau et al. (2010), Mori and Fujita (1982), Taylor and Christian (1967) and Staton-Bevan and Rawlings (1975).

4. Discussion and outlook

It is often assumed without further proof than matching experimental stress–strain curves that constitutive formulations are material invariant and can be applied to a range of materials with similar deformation mechanisms. For example, Taylor hardening has been employed to describe dislocation hardening in numerous materials. Similarly, we also assumed that the back stress formulation applies to a range of materials, which implies that the mechanics of dislocation structures apply across the materials studied. Our work further extended these notions by demonstrating that not only model forms but also model inputs can be material invariant. We have demonstrated that a unique set of mesoscale parameters associated with forest dislocation hardening in FCC materials can be identified for different materials that share similar dislocation structures. Since these parameters are known *a priori*, they effectively reduce testing needs and mitigate mesoscale modeling uncertainty, especially for cases in which single crystal data

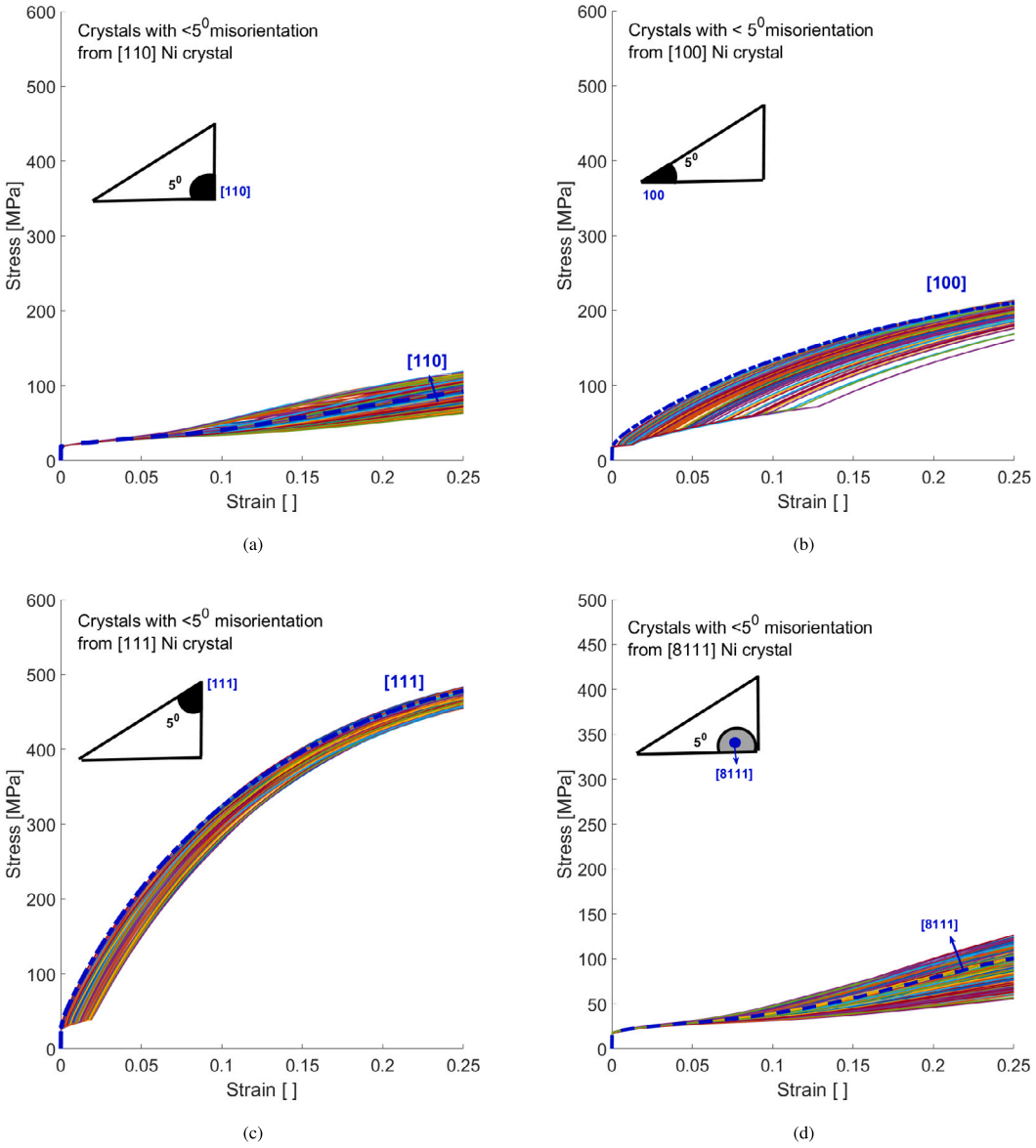


Fig. 7. Orientation sensitivity of stress–strain curves in different areas of inverse pole figure.

cannot be accessed. Hence, the approach is unique in matching single crystal response with pre-known mesoscale parameters for those FCC metals that share the same dislocation structures.

The novel sequential optimization approach calibrates parameters independently by analyzing simultaneously single crystal stress–strain curves from materials with similar dislocation structures (i.e., proxy materials). These parameters were used to predict the single crystal response of alloys such as stainless steel 316, NiCr, NiCo, and high entropy alloys. Hence, mesoscale attributes associated with forest dislocation hardening can be assumed to be material invariant to decrease significantly model input error. By leveraging on single crystal data from proxy materials we demonstrated that we can mitigate the parameter uncertainty more efficiently than performing a simultaneous optimization of all parameters with a single polycrystal test (e.g., compare the results in Figs. 1(b) and 5(a)). Moreover, disagreements with experiments in Fig. 5(a) can be used to identify sources of model form errors (e.g., missing grain size or texture effects). Hence, this work provides an opportunity to facilitate the use of CP model in industrial applications by drastically simplifying calibration while providing significant single crystal predictive power.

The notion of material invariant parameters may seem miraculous, and certainly, not all parameters fall in this category (e.g., parameters related to atomic unit processes such as glide activation energy). However, material invariance of dislocation structures has been established confidently from experiments (Sauzay and Kubin, 2011; Ashraf and Castelluccio, 2022). From the modeling perspective, the idea of parameter invariance has been previously exploited implicitly without much consideration. For

example, Bassani and Wu (1991) proposed a popular latent hardening matrix model for single crystals whose coefficients have been widely used by the community for numerous materials (Chouhan et al., 2023; Indurkar and Joshi, 2023; Zheng et al., 2023). This corresponds to an implicit use of material invariance related to dislocation hardening parameters that we formalize in this paper. Furthermore, our work supports the notion that CP models in general could present a degree of parameter material invariance given enough experimental data to identify parameters independently. Indeed, data-driven analysis (e.g., principal components analysis Wang et al., 2023) along with ample multi-material experimental datasets have the potential to identify clusters of parameters with low covariance across multiple materials. For example, novel approaches could determine the invariance character of a CP parameter using optimization weights that link specific mechanisms to parameters and data (e.g., cross-slip parameters in Step 2 could be calibrated to strong rolling textured polycrystals). Even the classical Chaboche model (Chaboche, 1989) could be redefined with a hybrid phenomenological/physics-based approach in which some of the back stresses correspond to material invariant contribution from forest dislocation hardening and do not need recalibration.

Our work has mainly focused on FCC metallic materials and can be directly applied to materials with similar structures. For example, ferrite has also been shown to follow the similitude principle with similar structures (Yalcinkaya et al., 2009) and could present material invariant parameters related to forest dislocation hardening. Notwithstanding, the sequential optimization strategy introduced for FCC materials can be reformulated for the different mechanisms in BCC and HCP materials to mitigate CP parameter uncertainty in these materials. Of course, even FCC engineering alloys have additional hardening mechanisms that are not material invariant (e.i., twinning, and phase transformations, etc.), but we argue that the current mesoscale parameterization may still describe dislocation hardening in those cases. For example, new optimization steps could be incorporated sequentially to calibrate parameters associated with known fractions of twinning or martensite (Wong et al., 2016) but without affecting the parameterizations of mesoscale dislocation structures. Hence, the overall uncertainty of a CP model with additional hardening mechanisms is enhanced by relying on the independent parameterization of forest dislocation strengthening presented in this contribution.

One final consideration with regards to size effects, which have been mostly ignored by considering macroscopic single crystals or polycrystals with a grain size of a few hundred microns. The CP formulation does not incorporate a grain size effect to avoid phenomenological equations without a rigorous parameterization strategy and physical interpretation (Yu et al., 2018). Hence, future work will explore the potential material-invariant character of crystal size effects, which has been found in experiments (Thangaraju et al., 2012).

5. Conclusions

This work explores model input uncertainty in CP models applied to FCC metals and alloys. Although we consider a specific CP model that was designed to account for the origin of each parameter independently, the conclusions are likely valid for other models and intrinsic material attributes. The results represent a significant step to facilitate the engineering use of CP models for FCC engineering alloys by drastically simplifying calibration, which is among the most pervasive barriers to adopting CP models for industrial applications. Moreover, we further enhance modeling confidence using parameterizations with proxy materials that extend mesoscale predictive power for single crystals, even when experimental data is not available for the specific alloy.

The novel hybrid physic-based/numerical optimization approach identifies parameters associated with mesoscale strengthening in FCC metallic materials. The approach determines sequentially parameters using single- or poly-crystal stress–strain curves and results in almost identical mesoscale parameters across multiple materials. Hence, we consider these parameters material-invariant and optimize them by combining stress–strain curves from different materials.

We also demonstrate that single-crystal stress–strain data are prone to larger experimental uncertainty than polycrystal data, which affects model uncertainty. As a result, calibrating CP models with single-crystal data from numerous materials and orientations is more effective in mitigating uncertainty compared to using fewer experiments from a single material.

Funding

GMC thanks The British Engineering and Physical Sciences Research Council (EPSRC) for the supporting funding under grant EP/R034478/1.

Code availability

The codes that support the findings of this study are available from the corresponding author upon reasonable request.

CRediT authorship contribution statement

Shahram Dindarlou: Writing – original draft, Software, Data curation. **Gustavo M. Castelluccio:** Writing – review & editing, Writing – original draft, Supervision, Methodology, Funding acquisition, Conceptualization.

Declaration of competing interest

The authors declare that they have no known competing financial interests or personal relationships that could have appeared to influence the work reported in this paper.

Data availability

Data will be made available on request.

Acknowledgment

GMC would like to thank Prof. David McDowell for the fruitful discussions and suggestions.

References

Akhtar, A., Teghtsoonian, E., 1971. Plastic deformation of Ni-Cr single crystals. Metall. Trans. 2 (10), 2757–2763.
Ashraf, F., Castelluccio, G., 2021. A robust approach to parameterize dislocation glide energy barriers in FCC metals and alloys. J. Mater. Sci. 56 (29), 16491–16509.
Ashraf, F., Castelluccio, G., 2022. On the similitude relation for dislocation wall thickness under cyclic deformation. Mater. Sci. Eng. A 142972.
Ashraf, F., Castelluccio, G., 2023. History and temperature dependent cyclic crystal plasticity model with material-invariant parameters. Int. J. Plast. 161, 103494.
Bassani, J., Wu, T., 1991. Latent hardening in single crystals II. Analytical characterization and predictions. PProc. R. Soc. Lond. Ser. A Math. Phys. Eng. Sci. 435 (1893), 21–41. http://dx.doi.org/10.1098/rspa.1991.0128.
Bertin, N., Capolungo, L., Beyerlein, I., 2013. Hybrid dislocation dynamics based strain hardening constitutive model. Int. J. Plast. 49, 119–144. http://dx.doi.org/10.1016/j.ijplas.2013.03.003, URL https://www.sciencedirect.com/science/article/pii/S0749641913000739.
Brahme, A., Inal, K., Mishra, R., Saimoto, S., 2011. The backstress effect of evolving deformation boundaries in FCC polycrystals. Int. J. Plast. 27 (8), 1252–1266.
Carreker, R., Hibbard, W., 1953. Tensile deformation of aluminum as a function of temperature, strain rate, and grain size. Acta Metall. 1 (6), 1157–1163. http://dx.doi.org/10.1016/0001-6160(53)90022-4.
Carter, C., Holmes, S., 1977. The stacking-fault energy of nickel. Philos. Mag.: A 35 (5), 1161–1172.
Castelluccio, G., McDowell, D., 2017. Mesoscale cyclic crystal plasticity with dislocation substructures. Int. J. Plast. 98, 1–26. http://dx.doi.org/10.1016/j.ijplas.2017.06.002.
Chaboche, J., 1989. Constitutive equations for cyclic plasticity and cyclic viscoplasticity. Int. J. Plast. 5 (3), 247–302. http://dx.doi.org/10.1016/0749-6419(89)90015-6, URL https://www.sciencedirect.com/science/article/pii/0749641989900156.
Chouhan, D., Mondal, S., Bhattacharya, B., Biswas, S., 2023. Role of slip and twinning on strain hardening, and correlation with geometric hardening, latent hardening, and grain boundary strengthening in titanium. Int. J. Plast. 161, 103516.
Devincre, B., Hoc, T., Kubin, L., 2008. Dislocation mean free paths and strain hardening of crystals. Science 1688, 61–64.
Devlin, J., 1974. Stacking fault energies of be, mg, al, cu, ag, and au. J. Phys. F: Metal Phys. 4 (11), 1865.
Dindarlou, S., Castelluccio, G., 2022. Substructure-sensitive crystal plasticity with material-invariant parameters. Int. J. Plast. 155.
Dunne, F., Rugg, D., Walker, A., 2007. Lengthscale-dependent, elastically anisotropic, physically-based hcp crystal plasticity: Application to cold-dwell fatigue in Ti alloys. Int. J. Plast. 23, 1061–1083.
El Shawish, S., Cizelj, L., 2017. Combining single-and poly-crystalline measurements for identification of crystal plasticity parameters: Application to austenitic stainless steel. Crystals 7 (6), 181.
Estrin, Y., Braasch, H., Brechet, Y., 1996. A dislocation density based constitutive model for cyclic deformation. J. Eng. Mater. Technol. 118 (4), 441–447. http://dx.doi.org/10.1115/1.2805940.
Feng, Z., Zecevic, M., Knezevic, M., Lebensohn, R.A., 2022. Predicting extreme anisotropy and shape variations in impact testing of tantalum single crystals. Int. J. Solids Struct. 241, 111466. http://dx.doi.org/10.1016/j.ijsolstr.2022.111466, URL https://www.sciencedirect.com/science/article/pii/S002076832200035X.
Follansbee, P., Gray, G., 1991. The response of single crystal and polycrystal nickel to quasistatic and shock deformation. Int. J. Plast. 7 (7), 651–660. http://dx.doi.org/10.1016/0749-6419(91)90049-5.
Gracio, J., Fernandes, J., Schmitt, J., 1989. Effect of grain size on substructural evolution and plastic behaviour of copper. Mater. Sci. Eng. A 118, 97–105. http://dx.doi.org/10.1016/0921-5093(89)90061-0.
Hansen, N., Huang, X., Winther, G., 2008. Grain orientation, deformation microstructure and flow stress. Mater. Sci. Eng. A 494 (1–2), 61–67.
He, J., Liu, W., Wang, H., Wu., Y., Liu, X., Nieh, T., Lu, Z., 2014. Effects of Al addition on structural evolution and tensile properties of the FeCoNiCrMn high-entropy alloy system. Acta Mater. 62, 105–113.
Heinrich, H., Neuhaus, R., Schwink, C., 1992. Dislocation structure and densities in tensile deformed Cu Mn crystals oriented for single glide. Phys. Status Solidi 131 (2), 299–308.
Herrera-Solaz, V., Llorca, J., Dogan, E., Karaman, I., Segurado, J., 2014. An inverse optimization strategy to determine single crystal mechanical behavior from polycrystal tests: Application to AZ31 Mg alloy. Int. J. Plast. 57, 1–15. http://dx.doi.org/10.1016/j.ijplas.2014.02.001.
Indurkar, P., Joshi, S., 2023. A mechanism-based multisurface plasticity model for hexagonal close-packed materials with detailed validation and assessment. J. Mech. Phys. Solids 176, 105302.
Karaman, I., Sehitoglu, H., Maier, H., Chumlyakov, Y., 2001. Competing mechanisms and modeling of deformation in austenitic stainless steel single crystals with and without nitrogen. Acta Mater. 49 (19), 3919–3933. http://dx.doi.org/10.1016/S1359-6454(01)00296-8.
Kashyap, B., Tangri, K., 1995. On the hall-petch relationship and substructural evolution in type 316L stainless steel. Acta Metall. Mater. 43 (11), 3971–3981.
Kawasaki, Y., 1974. Cell structures in deformed copper single crystals.
Kawasaki, Y., 1979. Correspondence between layered cell structures and slip lines in deformed copper single crystals. Japan. J. Appl. Phys. 18 (8), 1429–1438.
Kireeva, I., Chumlyakov, Y.I., Pobedennaya, Z., Platonova, Y.N., Kuksgauzen, I., Kuksgauzen, D., Poklonov, V., Karaman, I., Sehitoglu, H., 2016. Slip and twinning in the 1¯ 1 49-oriented single crystals of a high-entropy alloy. Russian Phys. J. 59, 1242–1250.
Kireeva, I., Chumlyakov, Y.I., Pobedennaya, Z., Vyrodova, A., Kuksgauzen, I., Kuksgauzen, D., 2018. Orientation and temperature dependence of a planar slip and twinning in single crystals of Al0. 3CoCrFeNi high-entropy alloy. Mater. Sci. Eng. A 737, 47–60.
Knoesen, D., Kritzinger, S., 1982. Dislocation cell boundary widths and dislocation cell sizes in deformed copper. Acta Metall. 30 (6), 1219–1222.
Kocks, U., UF, K., Argon, A., Ashby, M., 1975. Thermodynamics and kinetics of slip. Prog. Mater. Sci. 19, 1–47.
Kronmüller, H., 1959. Das magnetische einmündungsgesetz bei plastisch verformten nickel-und nickel-kobalt-einkristallen. Z. Phys. 154, 574–600.
Landau, P., Shneck, R., Makov, G., Venkert, A., 2010. In-situ TEM study of dislocation patterning during deformation in single crystal aluminum. In: Journal of Physics: Conference Series, vol. 241, IOP Publishing, 012060.
Langer, J., 2019. Statistical thermodynamics of crystal plasticity. J. Stat. Phys. 175 (3–4), 531–541. http://dx.doi.org/10.1007/s10955-019-02221-7.
Li, P., Li, S., Wang, Z., Zhang, Z., 2011. Fundamental factors on formation mechanism of dislocation arrangements in cyclically deformed fcc single crystals. Prog. Mater. Sci. 56 (3), 328–377. http://dx.doi.org/10.1016/j.pmatsci.2010.12.001.
Lodh, A., Keller, C., Castelluccio, G., 2023. Fabrication and mechanical testing of mesoscale specimens. JOM 1–7.
Marnier, G., Keller, C., Taleb, L., 2016. Fatigue of OFHC pure copper and 316L stainless steel subjected to prior tensile and cyclic prestrains. Int. J. Fatigue 91, 204–219. http://dx.doi.org/10.1016/j.ijfatigue.2016.06.009.

Mori, T., Fujita, H., 1982. Effect of dislocation structure on the flow stress in Cu-3 at.% Al single crystals. Phil. Mag. A 46 (1), 91–104.
Mukherjee, A., Mote, J., Dorn, J., 1965. Strain hardening of single aluminum crystals during polyslip. Trans. AIME.
Murr, L., 1973. Twin boundary energetics in pure aluminium. Acta Metall. 21 (6), 791–797.
Oberkampf, W.L., DeLand, S.M., Rutherford, B.M., Diegert, K.V., Alvin, K.F., 2002. Error and uncertainty in modeling and simulation. Reliab. Eng. Syst. Saf. 75 (3), 333–357. http://dx.doi.org/10.1016/S0951-8320(01)00120-X, URL https://www.sciencedirect.com/science/article/pii/S095183200100120X.
Pirgazi, H., Kestens, L., 2021. Semi in-situ observation of crystal rotation during cold rolling of commercially pure aluminum. Mater. Charact. 171, 110752. http://dx.doi.org/10.1016/j.matchar.2020.110752.
Pokharel, R., Lind, J., Kanjarla, A., Lebensohn, R., Li, S., Kenesei, P., Suter, R., Rollett, A., 2014. Polycrystal plasticity: comparison between grain-scale observations of deformation and simulations. Annu. Rev. Condens. Matter Phys. 5 (1), 317–346.
Roters, F., Eisenlohr, P., Hantcherli, L., Tjahjanto, D., Bieler, T., Raabe, D., 2010. Overview of constitutive laws, kinematics, homogenization and multiscale methods in crystal plasticity finite-element modeling: Theory, experiments, applications. Acta Mater. 58 (4), 1152–1211. http://dx.doi.org/10.1016/j.actamat.2009.10.058.
Rovinelli, A., Guilhem, Y., Proudhon, H., Lebensohn, R., Ludwig, W., Sangid, M., 2017. Assessing reliability of fatigue indicator parameters for small crack growth via a probabilistic framework. Modelling Simul. Mater. Sci. Eng. 25 (4), 045010.
Roy, C., Oberkampf, W., 2011. A comprehensive framework for verification, validation, and uncertainty quantification in scientific computing. Comput. Methods Appl. Mech. Engrg. 200 (25–28), 2131–2144.
Sangid, M., 2020. Coupling in situ experiments and modeling–opportunities for data fusion, machine learning, and discovery of emergent behavior. Curr. Opin. Solid State Mater. Sci. 24 (1), 100797.
Sard, R., Weil, R., 1970. Structure of electrodeposited copper single crystals—II. After plastic deformation. Electrochim. Acta 15 (12), 1991–1999.
Sauzay, M., Kubin, L., 2011. Scaling laws for dislocation microstructures in monotonic and cyclic deformation of fcc metals. Prog. Mater. Sci. 56 (6), 725–784. http://dx.doi.org/10.1016/j.pmatsci.2011.01.006.
Sauzay, M., Liu, J., Rachdi, F., Signor, L., Ghidossi, T., Villechaise, P., 2014. Physically-based simulations of the cyclic behavior of FCC polycrystals. Adv. Mater. Res. 891, 833–839.
Savage, D.J., Feng, Z., Knezevic, M., 2021. Identification of crystal plasticity model parameters by multi-objective optimization integrating microstructural evolution and mechanical data. Comput. Methods Appl. Mech. Engrg. 379, 113747. http://dx.doi.org/10.1016/j.cma.2021.113747, URL https://www.sciencedirect.com/science/article/pii/S0045782521000839.
Schramm, R., Reed, R., 1975. Stacking fault energies of seven commercial austenitic stainless steels. Metall. Trans. A 6, 1345–1351.
Sedighiani, K., Traka, K., Roters, F., Raabe, D., Sietsma, J., Diehl, M., 2022. Determination and analysis of the constitutive parameters of temperature-dependent dislocation-density-based crystal plasticity models. Mech. Mater. 164, 104117.
Staton-Bevan, A., Rawlings, R., 1975. Dislocation structures in deformed single-crystal Ni3 (Al, Ti). Phil. Mag. 32 (4), 787–800.
Steckmeyer, A., Sauzay, M., Weidner, A., Hieckmann, E., 2012. Micromechanical modelling of the cyclic stress–strain behaviour of nickel polycrystals. Int. J. Fatigue 40, 154–167.
Steeds, J., 1966. Dislocation arrangement in copper single crystals as a function of strain. Proc. R. Soc. Lond. Ser. A Math. Phys. Eng. Sci. 313, 509–529.
Sumino, K., Kawasaki, Y., Yamamoto, M., Sumino, M., 1963. Plastic deformation of foil copper crystals—II electron microscopical study. Acta Metall. 11 (11), 1235–1243.
Tagami, M., Kashihara, K., Okada, T., Inoko, F., 2001. Deformation structure and recrystallization in <111> aluminum single crystals deformed in tension at liquid nitrogen- and room-temperatures. J. Jpn. Inst. Metals 65 (8), 672–679. http://dx.doi.org/10.2320/jinstmet1952.65.8_672.
Takeuchi, T., 1975. Work hardening of copper single crystals with multiple glide orientations. Trans. Jpn. Inst. Metals 16 (10), 629–640.
Taylor, G., Christian, J., 1967. Experiments on the deformation of niobium single crystals: II. Electron microscope study of dislocation structures. Phil. Mag. 15 (137), 893–929.
Thangaraju, S., Heilmaier, M., Murty, B., Vadlamani, S., 2012. On the estimation of true hall–petch constants and their role on the superposition law exponent in Al alloys. Adv. Eng. Mater. 14 (10), 892–897.
Thompson, A., 1977. Effect of grain size on work hardening in nickel. Acta Metall. 25 (1), 83–86. http://dx.doi.org/10.1016/0001-6160(77)90249-8.
Veasna, K., Feng, Z., Zhang, Q., Knezevic, M., 2023. Machine learning-based multi-objective optimization for efficient identification of crystal plasticity model parameters. Comput. Methods Appl. Mech. Engrg. 403, 115740. http://dx.doi.org/10.1016/j.cma.2022.115740, URL https://www.sciencedirect.com/science/article/pii/S0045782522006958.
Venkatesan, P., Beshers, D., 1970. Plastic deformation in nickel crystals. Metall. Trans. 1 (6), 1780–1782.
Venkatraman, A., McDowell, D.L., Kalidindi, S.R., 2022. Bayesian analysis of parametric uncertainties and model form probabilities for two different crystal plasticity models of lamellar grains in $\alpha + \beta$ titanium alloys. Int. J. Plast. 154, 103289. http://dx.doi.org/10.1016/j.ijplas.2022.103289, URL https://www.sciencedirect.com/science/article/pii/S0749641922000717.
Wang, J., Zhu, B., Hui, C.-Y., Zehnder, A.T., 2023. Determination of material parameters in constitutive models using adaptive neural network machine learning. J. Mech. Phys. Solids 177, 105324. http://dx.doi.org/10.1016/j.jmps.2023.105324, URL https://www.sciencedirect.com/science/article/pii/S002250962300128X.
Wong, S.L., Madivala, M., Prahl, U., Roters, F., Raabe, D., 2016. A crystal plasticity model for twinning- and transformation-induced plasticity. Acta Mater. 118, 140–151. http://dx.doi.org/10.1016/j.actamat.2016.07.032, URL https://www.sciencedirect.com/science/article/pii/S1359645416305407.
Yalcinkaya, T., Brekelmans, W., Geers, M., 2009. A composite dislocation cell model to describe strain path change effects in BCC metals. Modelling Simul. Mater. Sci. Eng. 17 (6), 064008.
Yu, C., Kang, G., Kan, Q., 2018. A micromechanical constitutive model for grain size dependent thermo-mechanically coupled inelastic deformation of super-elastic NiTi shape memory alloy. Int. J. Plast. 105, 99–127. http://dx.doi.org/10.1016/j.ijplas.2018.02.005, URL https://www.sciencedirect.com/science/article/pii/S074964191730606X.
Zheng, Z., Xie, C., Chen, J., Huang, Z., 2023. A crystal plasticity model of low cycle fatigue damage considering dislocation density, stress triaxiality and lode parameter. Int. J. Fatigue 175, 107823.



https://dspace.org/

Optimization of crystal plasticity parameters with proxy materials data for alloy single crystals

Dindarlou, Shahram; Castelluccio, Gustavo M.

2024-03-01
Elsevier
https://doi.org/10.1016/j.ijplas.2024.103894
Dindarlou S, Castelluccio GM. (2024) Optimization of crystal plasticity parameters with proxy materials data for alloy single crystals. International Journal of Plasticity, Volume 174, March 2024, Article number 103894

Downloaded from a DSpace repository. https://dspace.org/